




Majorana bound state in the continuum: Coupling between a Majorana bound state and a quantum dot mediated by a continuum energy spectrum

J. P. Ramos-Andrade ^{1,2,*}, P. A. Orellana ¹ and E. Vernek ^{2,3}

¹*Departamento de Física, Universidad Técnica Federico Santa María, Casilla 110 V, Valparaíso, Chile*

²*Instituto de Física, Universidade Federal de Uberlândia, Uberlândia, Minas Gerais 38400-902, Brazil*

³*Department of Physics and Astronomy, and Nanoscale and Quantum Phenomena Institute, Ohio University, Athens, Ohio 45701-2979, USA*



(Received 9 September 2019; revised manuscript received 3 February 2020; accepted 12 February 2020; published 2 March 2020)

A quantum dot (QD) coupled to topological quantum wires is fertile ground to explore the physical properties of Majorana bound states (MBSs). We consider a single-level QD and a MBS, both coupled to an electron reservoir with a continuum energy spectrum. By increasing the coupling between the MBS and the metallic contact, the MBS leaks into the continuum, modifying the local spectral properties of the QD either in the noninteracting or the Coulomb blockade regimes. Surprisingly, regardless of the strength of the coupling between the MBS and the continuum, the Majorana states always appear as a bound state, as long as the QD level is resonant with the Fermi level. By applying a gate voltage in the system, we can control the QD level position while leaving the MBS pinned to the Fermi level. This provides an interesting way to explore the physical properties of this peculiar bound state in the continuum.

DOI: [10.1103/PhysRevB.101.115403](https://doi.org/10.1103/PhysRevB.101.115403)

I. INTRODUCTION

The progress of theoretical formulations and experimental techniques in condensed matter physics provides an interesting playground for scientists to investigate intriguing phenomena at low energy, commonly associated with elementary particles that would be possible solely in high energy physics [1]. An example is the possibility to observe Majorana bound states (MBSs) that have similarities with the original Majorana fermion, an exotic elementary particle predicted many years ago [2]. In condensed matter, MBSs are predicted to emerge as collective excitations in p -wave topological superconductors (TSC) [3–5]. MBSs satisfy non-Abelian statistics which have produced a great deal of excitement because of its potential applications in quantum computation [6–9]. After the theoretical proposal performed by Kitaev [10], in which MBSs would emerge bound to edges of a one-dimensional (1D) TSC [11], several experiments have carried out the physical realization of the Kitaev model, finding signatures of their presence through anomalies in physical quantities measurement [12–18]. Nowadays, interest in MBSs can be classified from two distinct (nonexclusive) perspectives: (1) The search for an ultimate scheme to detect MBSs, which despite the number of recent experiments remains under debate, and (2) the design of reliable platforms for manipulation of MBSs, envisioning future technological applications as in non-Abelian quantum computation [19]. Indeed, from these early physical realizations to practical use, a long road still has to be paved. In this context, the behavior of MBSs in nanoscopic systems such as hybrid topological

wires-quantum dot (QD) structures has recently gained considerable attention [20].

Owing to the great flexibility to control their electronic properties, QDs have proven to be a convenient platform to study MBSs in condensed matter [21–26]. A first system to detect MBS composed of a QD coupled to topological wire was suggested by Liu and Baranger [27]. Two normal metallic contacts also coupled to the QD served as a source and drain used to calculate the conductance across the QD-MBS structure. A striking half-integer conductance was obtained across the junction when a single MBS was coupled to the QD. Later on, it was shown that this feature is obtained regardless of the QD energy level, resulting in a leaking of a MBS [28] into the QD. In fact this leaking phenomena was later observed experimentally [17].

In the setup discussed above, the MBS leaked into the QD because they were directly coupled to each other. The reader may ask what would happen if the Majorana mode were not directly coupled to the dot. Furthermore, what features will appear if the mediation is performed through a typical experimental feature, such as a continuum of states. Our results show that regardless of the MBS-continuum coupling strength, the bound state character of the latter remains unchanged [29]. As such, as far as the MBS *plus* the contacts is concerned, this problem can be viewed as a bound state in the continuum (BIC) akin to the prediction by von Neumann and Wigner in a generic framework of engineered potential [30] and later studied in many fermion systems (see Ref. [31] and references therein). However, this bound state does not represent a full fermion, as in the traditional case, it rather corresponds to a MBS or “half fermion,” as it is commonly referred. Hence, we refer to this state as Majorana bound state in the continuum (MBIC). Recently, BICs have gained

*juan.ramosa@usm.cl

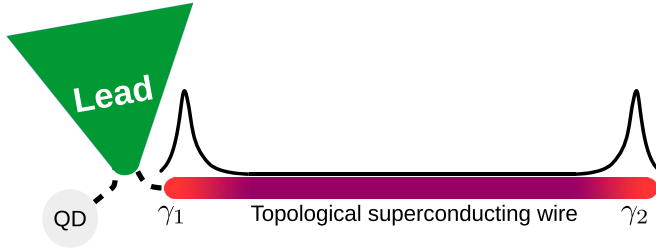


FIG. 1. Schematic representation of the model: A single level QD (gray) and a TSW, hosting MBSs (orange) γ_1 and γ_2 at its ends, coupled to a common metallic lead (green) with a continuum spectrum. The black curve above the topological wire represents the wave function associated to the Majorana bound states (note the peaks at the ends).

considerable attention as they have been observed in photonic systems. Also, motivated by the interference phenomena taking place in electronic systems in analogy with the photonic counterpart, the presence of BICs promoted by MBS has been studied [32,33]. Similarly, interplay between MBSs and BICs has been proposed as a useful tool to perform applications in quantum computing, allowing, for instance, to read/write information through veiling/unveiling these states [34–36]. Indeed, MBSs provide a quite attractive way to produce BICs as they are topologically protected against local perturbations [37,38]. As a result, manipulating electronic properties of QDs becomes much more suitable, given that the rest of the system turns out to be almost insensitive to applied electric fields.

In this work, we propose to study the electronic properties of a system composed of a QD and a topological superconducting wire (TSW), both connected to a common metallic contact. The TSW is assumed to be in its topological phase, holding MBSs at its ends, as the system is schematically depicted in Fig. 1. Alternatively, this system can be viewed as a QD coupled to an effective continuum exhibiting an MBSs. By employing the Green's function method and the equation of motion techniques, we study the spectral and transport properties of the system. While in the noninteracting regime of the QD, we can access the physical properties exactly; in its interacting regime, they are available only under certain approximation. Here, we employ the so-called Hubbard I approximation that is known to capture qualitatively well the many-body physics in the Coulomb blockade regime [39]. Our results show that no matter how strong the MBS is coupled to the continuum, the QD spectral function always shows it as a bound state. This behavior remains unchanged in the strong Coulomb interaction regime of the QD.

This paper is organized as follows: Section II presents the system Hamiltonian and method used to obtain quantities of interest; Sec. III shows the corresponding results and the related discussion. Finally, our concluding remarks are presented in Sec. IV.

II. HAMILTONIAN MODEL AND METHOD

For the sake of completeness, the system under study consists of a QD and an MBS located at the end of a TSW, both connected with a common normal metallic lead, as schematically shown in Fig. 1. The Hamiltonian of the system

can be written as

$$H = H_c + H_{\text{dot}} + H_{c\text{-dot}} + H_{c\text{-MBS}}, \quad (1)$$

where the first three terms of Eq. (1) correspond to the traditional Anderson Hamiltonian describing the QD plus the normal metallic lead and are given by

$$H_c = \sum_{\mathbf{k}, \sigma} \varepsilon_{\mathbf{k}} c_{\mathbf{k}, \sigma}^\dagger c_{\mathbf{k}, \sigma}, \quad (2)$$

$$H_{\text{dot}} = \sum_{\sigma} \varepsilon_d d_{\sigma}^\dagger d_{\sigma} + U n_{\uparrow} n_{\downarrow}, \quad (3)$$

$$H_{c\text{-dot}} = \sum_{\mathbf{k}, \sigma} (V_{\mathbf{k}} c_{\mathbf{k}, \sigma}^\dagger d_{\sigma} + V_{\mathbf{k}}^* d_{\sigma}^\dagger c_{\mathbf{k}, \sigma}), \quad (4)$$

where $c_{\mathbf{k}, \sigma}^\dagger$ ($c_{\mathbf{k}, \sigma}$) creates (annihilates) a continuum electron with momentum \mathbf{k} and spin σ ; d_{σ}^\dagger (d_{σ}) does it in the QD with energy level ε_d , U is the electron-electron interaction, $n_{\sigma} = d_{\sigma}^\dagger d_{\sigma}$ is the number operator, and $V_{\mathbf{k}}$ represents the tunneling matrix element between the continuum states and the QD orbitals. The last term in Eq. (1) describes the coupling between the MBS and the lead and is given by [27]

$$H_{c\text{-MBS}} = \sum_{\mathbf{k}} \lambda (c_{\mathbf{k}, \downarrow} - c_{\mathbf{k}, \downarrow}^\dagger) \gamma_1, \quad (5)$$

in which λ represents the real coupling parameter and γ_1 the MBS operator, which satisfy both $\gamma_1^\dagger = \gamma_1$ and $\gamma_1^2 = 1$. We have assumed that the Majorana mode is provided by a long TSW that are fully polarized with spin *down* by an effective magnetic field along the z direction. Hence only electrons with spin *down* couple to the MBS. Moreover, it is worth mentioning that we consider a TSW in the long-wire limit, then the MBS placed at the opposite end, γ_2 , is strictly equivalent to γ_1 .

We are interested in studying the influence of the MBS on the physical properties of the QD, mediated by the continuum. To access the relevant physical quantities we employ the Green's function formalism, which allows us to obtain, for instance, the spin-resolved local density of states (LDOS) at the QD, $\rho_{d, \sigma}(\varepsilon)$ and transport properties. In terms of the Green's function (GF), the spin dependent LDOS is given by

$$\rho_{d, \sigma}(\varepsilon) = -\frac{1}{\pi} \text{Im}[\langle\langle d_{\sigma}; d_{\sigma}^\dagger \rangle\rangle_{\varepsilon}], \quad (6)$$

where $\langle\langle d_{\sigma}; d_{\sigma}^\dagger \rangle\rangle_{\varepsilon}$ denotes the spin-resolved retarded GF of the QD in energy domain. In the following, we will address the model either in the noninteracting ($U = 0$) or interacting ($U > 0$) cases. For $U > 0$, it is known that one cannot obtain an exact expression for the GF. However, approximations can still be obtained. For instance, the so-called Hubbard I approximation is known to provide a fairly good description of Coulomb blockade phenomena above the Kondo temperature. Such an expression can be derived by using the equation-of-motion technique, as discussed in Appendix. Within this approximation, the GF acquires the form

$$\begin{aligned} & \langle\langle d_{\sigma}; d_{\sigma}^\dagger \rangle\rangle_{\varepsilon} \\ &= \frac{\varepsilon - \varepsilon_d - U(1 - \langle n_{\bar{\sigma}} \rangle)}{(\varepsilon - \varepsilon_d)(\varepsilon - \varepsilon_d - U) - (\varepsilon - \varepsilon_d - U(1 - \langle n_{\bar{\sigma}} \rangle))\Sigma_{\sigma}(\varepsilon)}, \end{aligned} \quad (7)$$

in which

$$\Sigma_{\uparrow}(\varepsilon) = -i\Gamma, \quad (8a)$$

$$\Sigma_{\downarrow}(\varepsilon) = -i\frac{\Gamma}{1 - M(\varepsilon)} \quad (8b)$$

are the spin-resolved self-energies of the QD. In the above, $\langle n_{\sigma} \rangle$ is the occupation of the QD for a given spin σ and

$$M(\varepsilon) = -2i\Lambda \left[\varepsilon + \frac{2i\Lambda(\varepsilon + \varepsilon_d)(\varepsilon + \varepsilon_d + U)}{(\varepsilon + \varepsilon_d)(\varepsilon + \varepsilon_d + U) + i\Gamma(\varepsilon + \varepsilon_d + U(1 - \langle n_{\uparrow} \rangle))} \right]^{-1}, \quad (9)$$

where $\Lambda = \pi\lambda^2/2D$ is the hybridization strength between the MBS and the continuum. Since the GF in Eq. (7) depends on the occupation, it must be determined self-consistently.

III. NUMERICAL RESULTS

To show our numerical results, let us set the hybridization Γ as the energy unit. In the following, we will analyze the LDOS as a function of the energy for different values of the relevant parameters of the system, Λ , ε_d and U . We will first discuss the result in the noninteracting case, $U = 0$, and next we will address the case of $U \neq 0$.

A. Noninteracting quantum dot ($U = 0$)

For $U = 0$, the expression for the GF [Eq. (7)] becomes exact and acquires the form

$$\langle\langle d_{\sigma}; d_{\sigma}^{\dagger} \rangle\rangle_{\varepsilon} = \frac{1}{\varepsilon - \varepsilon_d - \Sigma_{\sigma}(\varepsilon)}. \quad (10)$$

The effect of the MBS in the QD is accounted for by the self-energy Σ_{\downarrow} , via

$$M(\varepsilon, U = 0) = -2i\Lambda \left[\varepsilon + 2i\Lambda \frac{\varepsilon + \varepsilon_d}{\varepsilon + \varepsilon_d + i\Gamma} \right]^{-1}. \quad (11)$$

Note that since the electron's spins are decoupled from each other, the spin \uparrow component is not affected by the MBS. Therefore, we focus only on the electrons with spin \downarrow in the QD. As usual, the self-energy encompasses the information from the rest of the system by shifting the energy level of the QD by an amount $\text{Re}[\Sigma_{\downarrow}(\varepsilon)]$ and broadening the bare level by a quantity $-\text{Im}[\Sigma_{\downarrow}(\varepsilon)] \equiv \Gamma_{\text{eff}}(\varepsilon)$. The latter represents the effective hybridization between the QD and continuum, modified by the MBS. For $\lambda \rightarrow 0$, $\Gamma_{\text{eff}} \rightarrow \Gamma$, that is independent of ε .

In Fig. 2 we show $\text{Re}[\Sigma_{\downarrow}(\varepsilon)]$ and $\Gamma_{\text{eff}}(\varepsilon)$ as a function of ε , using $\varepsilon_d = 0$ and different values of Λ . First of all, it is interesting noting in Fig. 2(a) that $\Gamma_{\text{eff}}(\varepsilon = 0) = 0$ for any value of $\Lambda \neq 0$. This is somewhat surprising because it results from a destructive quantum interference—involving a “half” fermion—and is very much similar to the case of a conventional fermion in the continuum. This complete antiresonance at $\varepsilon = 0$ decouples the electrons with spin \downarrow of the QD from the continuum. For $|\varepsilon| \gg \Gamma$ we note that Γ_{eff} tends to saturate at different values depending on how big Λ is. This can be understand analytically. In the limit $\Lambda/\Gamma \gg 1$ and $\varepsilon_d = 0$,

$\Gamma = (\pi V^2/2D)\Theta(D - |\omega|)$ (with D being the bandwidth of the metallic contact) represents the energy-independent hybridization parameter between the continuum and QD, which is derived in the wide-band limit (D much larger than any other energy parameter of the system). Note that $\Sigma_{\downarrow}(\varepsilon)$ is modified by the presence of the MBSs accounted by the function $M(\varepsilon)$, which is given by (see Appendix)

Eq. (11) leads to

$$\Gamma_{\text{eff}}(\varepsilon, \varepsilon_d = 0) = \frac{\Gamma}{2} \frac{\varepsilon^2}{\varepsilon^2 + (\Gamma/2)^2}, \quad (12)$$

which is independent of Λ . From this equation it is easy to see that for energies $|\varepsilon| \gg \Gamma$ we obtain $\Gamma_{\text{eff}} = \Gamma/2$.

In Fig. 2(b) we show the real part of the self energy. Note that, by virtue of the wide-band limit, $\text{Re}[\Sigma_{\downarrow}(\varepsilon)] = 0$ for $\Lambda = 0$. Moreover, $\text{Re}[\Sigma_{\downarrow}(\varepsilon = \varepsilon_d = 0)] = 0$ for any value of Λ and becomes finite for $\varepsilon \neq 0$, but restricted to the condition $|\text{Re}[\Sigma_{\downarrow}(\varepsilon)]| < \Gamma/2$.

In Fig. 3 we show $\Sigma_{\downarrow}(\varepsilon)$ for fixed Λ and different $\varepsilon_d > 0$. In Fig. 3(a) we see that Γ_{eff} vanishes only for $\varepsilon_d = 0$. Moreover, we note that $\Gamma_{\text{eff}}(\varepsilon = 0) \rightarrow \Gamma/2$ for large ε_d . This is a remarkable signature of the presence of the Majorana zero mode in the continuum. In the limit $\varepsilon_d \gg \Gamma$, the contribution given by the MBS to Γ_{eff} is $M(\varepsilon; U = 0) = 2i\Lambda[\varepsilon + 2i\Lambda]^{-1}$. With this we obtain

$$\Gamma_{\text{eff}}(\varepsilon, \varepsilon_d \gg \Gamma) = \Gamma \left(\frac{\varepsilon^2}{\varepsilon^2 + 16\Lambda^2} + \frac{8\Lambda^2}{\varepsilon^2 + 16\Lambda^2} \right). \quad (13)$$

This clearly shows that $\Gamma_{\text{eff}} = \Gamma/2$ as $\varepsilon \rightarrow 0$ regardless the value of Λ . Interestingly, similar to what was observed

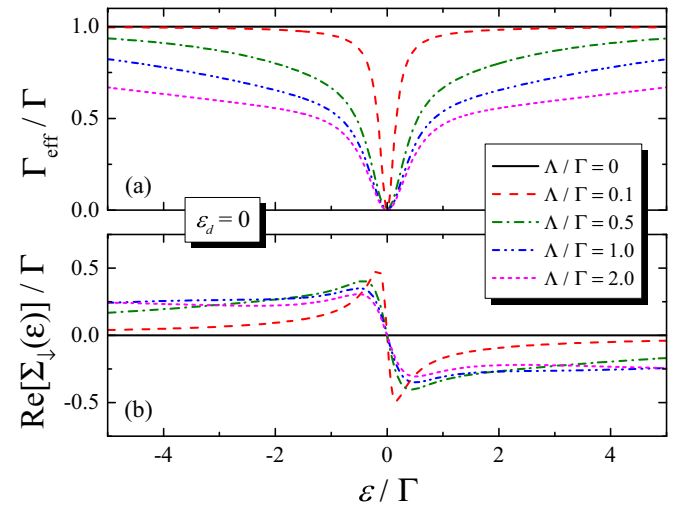


FIG. 2. (a) Γ_{eff} and (b) $\text{Re}[\Sigma_{\downarrow}(\varepsilon)]$ as a function of the energy for different MBS-lead couplings Λ . Here, the QD energy level is fixed at $\varepsilon_d = 0$. The flat solid black curve for $\Lambda = 0$ reflects the wide band limit assumed in the calculations.

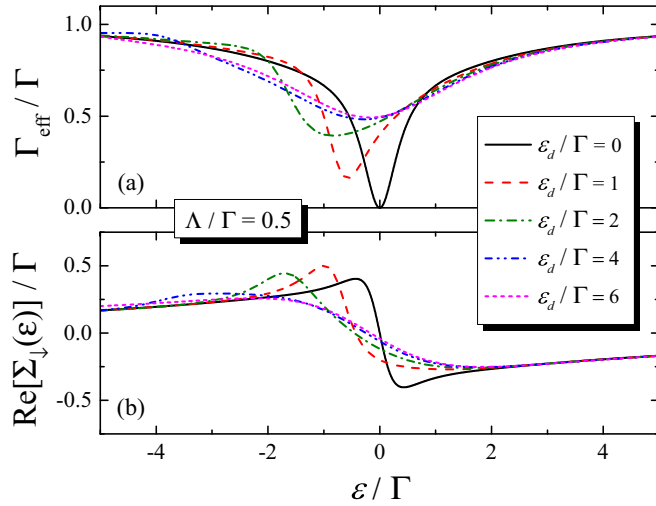


FIG. 3. (a) Γ_{eff} and (b) $\text{Re}[\Sigma_{\downarrow}(\varepsilon)]$ as a function of the energy for different QD energy levels ε_d . Here, the MBS-continuum coupling is fixed at $\Lambda/\Gamma = 0.5$. Note that in (a) Γ_{eff} vanishes only for $\varepsilon_d = 0$.

in Fig. 2(b), in Fig. 3(b) $\text{Re}[\Sigma_{\downarrow}(\varepsilon)]$ is also limited as $|\text{Re}[\Sigma_{\downarrow}(\varepsilon)]| < \Gamma/2$.

The behavior of the self-energy discussed above has important consequences in the QD LDOS, $\rho_d(\varepsilon)$, calculated from Eq. (6). This quantity is the one that is actually accessible in experiments via transport spectroscopy. Figure 4(a) shows LDOS as a function of ε and Λ for $\varepsilon_d = 0$. For $\Lambda = 0$ (uncoupled MBS), we observe a broad peak placed around $\varepsilon = \varepsilon_d = 0$. Once the coupling of the MBS is turned on ($\Lambda \neq 0$), the amplitude of the LDOS decreases as Λ increases, but the height of the peak does not go below $1/2\pi\Gamma$. Besides, at $\varepsilon = 0$ a sharp peak is observed. This sharp peak is a direct consequence of the vanishing effective hybridization function due to the presence of the MBIC. It is better appreciated in Fig. 4(b) where we show ρ_d along the horizontal orange lines of Fig. 4(a). Indeed, this behavior can be understood analytically; from Eq. (10), in the limit of strong MBS coupling ($\Lambda \gg \Gamma$), we can write

$$\pi\rho_d(\varepsilon, \varepsilon_d = 0) = \frac{\Gamma}{2} \left(\frac{1}{\varepsilon^2 + \Gamma^2} \right) + \frac{\pi}{2} \delta(\varepsilon). \quad (14)$$

Clearly, at $\varepsilon_d = 0$ a bound state in the continuum is obtained at zero energy whenever $\Lambda \neq 0$. In Fig. 4(c) ρ_d is displayed for fixed $\Lambda \gg \Gamma$ and different values of $\varepsilon_d \neq 0$. Note that the observed MBIC feature evolves to a situation with an antiresonance at $\varepsilon = \varepsilon_d$ for $\varepsilon_d \neq 0$. Analytically, for small values of ε_d , as in Fig. 4(c), we can approximate the LDOS as

$$\pi\rho_d(\varepsilon) \sim \frac{\Gamma}{2} \frac{(\varepsilon + \varepsilon_d)^2}{(\varepsilon - \varepsilon_d)^4 + \varepsilon^2\Gamma^2}. \quad (15)$$

From this, we note that indeed there is an antiresonance at $\varepsilon = \varepsilon_d$. We see, therefore, that tuning ε_d is relevant to achieve a MBIC. At this point, we should emphasize that in this noninteracting scenario, MBIC seen in the QD LDOS results solely from the leaking of the MBS into the continuum. In the following, we will see that this feature is still present in the interacting regime of the QD.

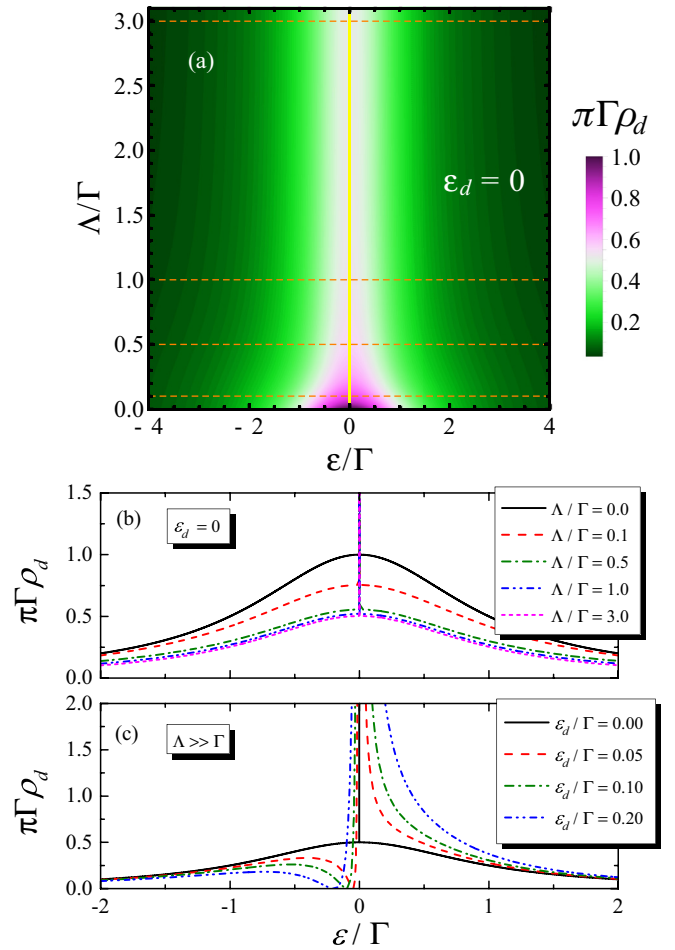


FIG. 4. (a) Color map of LDOS in the QD, ρ_d , as function of the energy and Λ . The vertical solid yellow line represents the δ -Dirac function $\delta(\varepsilon)$. ρ_d as a function of energy (b) for different Λ values using $\varepsilon_d = 0$, and (c) for different ε_d values using $\Lambda \gg \Gamma$. In panel (b), the curves with $\Lambda \neq 0$ correspond to the horizontal dashed orange lines in panel (a).

B. Interacting regime

In this subsection we study the interacting regime of the QD, $U \neq 0$. We focus on the Coulomb blockade regime, to which the Hubbard approximation is reasonably good. In contrast to the previous subsection, now the LDOS depends on the temperature T , and we use T larger than the Kondo temperature T_K so that Kondo correlations are thermally suppressed. According to the parameters in our model, the Kondo temperature is estimated using Haldane expression [40], such as $k_B T_K \sim 0.018\Gamma$. Here we should emphasize that, as a consequence of the Coulomb interaction, the GF for spin σ [Eq. (7)] depends on QD occupation $\langle n_{\bar{\sigma}} \rangle$ given by

$$\langle n_{\sigma} \rangle = -\frac{1}{\pi} \int_{-\infty}^{\infty} d\varepsilon \text{Im}[\langle \langle d_{\sigma}; d_{\sigma}^{\dagger} \rangle \rangle_{\varepsilon}] f(\varepsilon), \quad (16)$$

where $f(\varepsilon)$ is the Fermi's function. Therefore, it forces us to perform a self-consistent calculation numerically. To show our numerical result, we set $U = 10\Gamma$ and carry on the numerical calculations at $k_B T = 6 \times 10^{-2}\Gamma$ which happens to be above $k_B T_K$ for most of the parameters used throughout this paper.

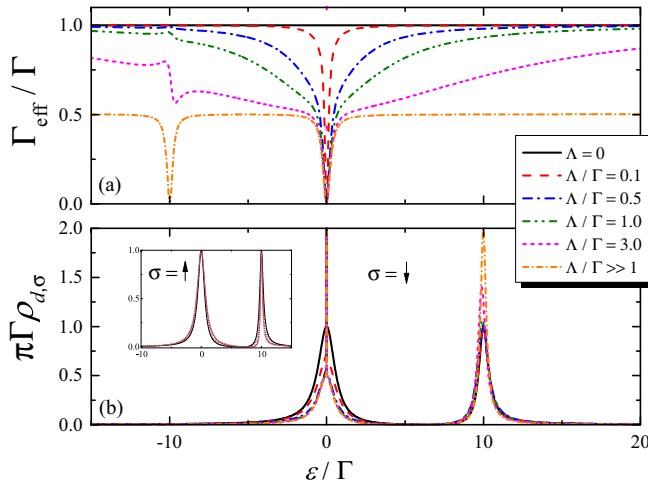


FIG. 5. (a) Γ_{eff} and (b) LDOS for spin $\sigma = \downarrow$ as a function of the energy for different Λ . The inset in panel (b) is the LDOS for spin $\sigma = \uparrow$.

In Fig. 5 we show the effect of the MBS in the effective hybridization function [Fig. 5(a)] and the LDOS [Fig. 5(b)] for a fixed $\varepsilon_d = 0$ and various values of Λ . Figure 5(a) is similar to what is displayed in Fig. 2(a), but now for finite U . We observe that $\Gamma_{\text{eff}} = \Gamma$ for $\Lambda = 0$ and $\Gamma_{\text{eff}} = 0$ for $\varepsilon = \varepsilon_d = 0$, whenever $\Lambda \neq 0$. This behavior is very similar to the noninteracting case shown in Fig. 2(a). Again, this is a direct consequence of the MBS leaking into the continuum, reaching the physics quantities in the QD. The behavior of the curves of Fig. 5(a) can be obtained analytically from Eq. (9) for large values of Λ . In fact, for $\Lambda \gg \Gamma$, $M(\varepsilon)$ it is independent of Λ .

$$\pi \rho_{d,\downarrow}(\varepsilon) = \frac{\Gamma}{2} \frac{(\varepsilon + U)^2 (\varepsilon - (1 - \langle n_{\uparrow} \rangle) U)^2}{\varepsilon^6 + (1 - \langle n_{\uparrow} \rangle)^2 U^4 \Gamma^2 + \varepsilon^4 (\Gamma^2 - 2U^2) + \varepsilon^2 U^2 (U^2 - 2(1 - \langle n_{\uparrow} \rangle) \Gamma^2)} + \frac{\pi}{3} \delta(\varepsilon). \quad (18)$$

Despite the complexity of the equation above, for the corresponding occupancy, we can extract that the wide peak placed around $\varepsilon = 0$ asymptotically reaches $\pi \rho_{d,\downarrow} \rightarrow 1/2\Gamma$, while the one located at $\varepsilon = U$ increases up to $\pi \rho_{d,\downarrow} \rightarrow 2/\Gamma$, both in the limit $\Lambda \gg \Gamma$.

Before closing this section, we show how the presence of the MBIC affects the occupation of the QD. In Fig. 6, we show the spin-resolved occupation number in the QD as a function of ε_d . From this figure, for $\Lambda = 0$ (solid black lines) there is spin degeneration in the occupancy, as we expected since the Hamiltonian is spin symmetric for this case. Allowing coupling between the MBS and the continuum, $\Lambda \neq 0$, the spin symmetry brakes, and deviations are observed. As a consequence, in Fig. 6(a) we observe a subtle oscillation of n_{\uparrow} around $\varepsilon_d = 0$ and $\varepsilon_d = -U$, better seen in the inset for energies near $\varepsilon_d = 0$. In Fig. 6(b) we show the corresponding curves for n_{\downarrow} . Here, a more interesting consequence of the MBS is visible. Note that, while for $\Lambda = 0$ the occupancy always increases as we decrease ε_d (same happening to $\langle n_{\uparrow} \rangle$), for finite Λ $\langle n_{\downarrow} \rangle$ decreases with ε_d within the interval $-U < \varepsilon_d < 0$. By noting that for a given ε_d in this interval, $\langle n_{\downarrow} \rangle$ decreases while $\langle n_{\uparrow} \rangle$ increases as Λ increases, we conclude

In this limit, setting $\varepsilon_d = 0$, we can write the effective hybridization as

$$\Gamma_{\text{eff}}(\varepsilon) = \frac{2\Gamma\varepsilon^2(\varepsilon + U)^2}{4\varepsilon^2(\varepsilon + U)^2 + [\varepsilon + (1 - \langle n_{\uparrow} \rangle)U]^2\Gamma^2}. \quad (17)$$

This result clearly shows that $\Gamma_{\text{eff}} = 0$ vanishes at both $\varepsilon = 0$ and $\varepsilon = -U$. Nevertheless, no important consequence in the $\rho_{d,\sigma}$ is observed for $\varepsilon_d = -U$, since that energy is far away from the $\varepsilon_d = 0$. Similarly to the noninteracting case, we note also that $\Gamma_{\text{eff}} \rightarrow \Gamma/2$ for all the energies regions such as $|\varepsilon| \gg \Gamma, U$.

The features observed for Γ_{eff} are directly related to the LDOS of the QD, which is shown in Fig. 5(b). For the case with unconnected MBSs, $\Lambda = 0$, two peaks are observed, of the same amplitude, localized at energies $\varepsilon = 0$ and $\varepsilon = U$ due to the Coulomb blockade regime in our system. On the other hand, for the cases with $\Lambda \neq 0$, different modifications are achieved in each of the mentioned peaks. The amplitude of the peak located around $\varepsilon = 0$ decreases as Λ increases, while at exactly $\varepsilon = 0$ a very narrow peak, a MBIC, arises from the QD effective disconnection ($\Gamma_{\text{eff}}(\varepsilon = \varepsilon_d = 0) = 0$), which is similar to the one discussed in Sec. III A. At this point, it is interesting to note that the peak located at $\varepsilon = U$ becomes narrower and increases its amplitude, although it remains finite since Γ_{eff} does not vanish. Thus, whenever the QD is in the Coulomb regime, the leaked MBS into the continuum affects the LDOS substantially, in a similar fashion as in the noninteracting case.

Taking into account the discussion above, the LDOS for the QD for spin *down* can be written as

that there is a spin polarization in the QD. It can be interpreted as an effective magnetic field due to the presence of the MBS that breaks the time-reversal symmetry of the system.

IV. CONCLUSIONS

We studied a system formed by a QD coupled to the continuum, which is connected to an MBS localized at the end of a TSW. Considering that continuum electrons with a particular spin *down* couple to the MBS, we found that the leakage of the MBS into the continuum affects the physical properties of the QD greatly. As a consequence of this leaking, the QD becomes effectively decoupled from the rest of the system at energies $\varepsilon = \varepsilon_d = 0$, for both interacting and noninteracting regimes. In the interacting case, the second peak due to Coulomb blockade, placed at $\varepsilon = \varepsilon_d + U$, is also affected by the MBIC. It becomes narrower and increases its amplitude as the coupling strength between MBS and continuum increases. Besides, we have performed an analytic treatment of the effective coupling and LDOS in the limit of strong MBS-continuum coupling. Owing to the robustness of the MBS against the applied electric field, MBICs provide

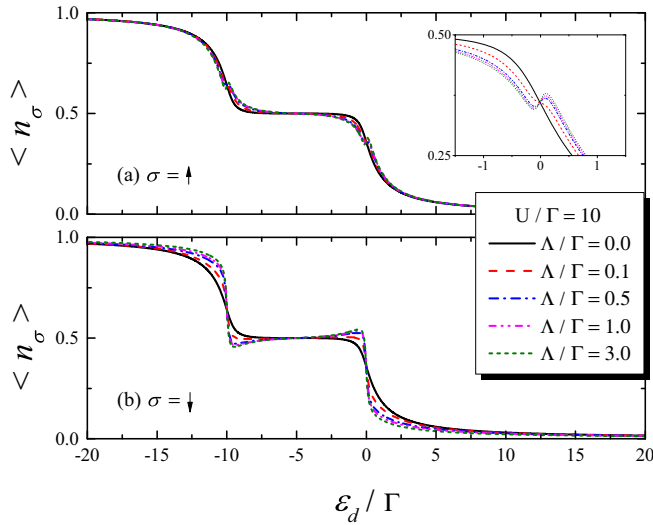


FIG. 6. Occupation number (a) n_\uparrow and (b) n_\downarrow of the QD as function of ε_d , for different Λ values. The inset of panel (a) shows a zoomed n_\uparrow around $\varepsilon_d = 0$.

an exciting way to control the QDs electronic properties without changing the energy position of the bound state in the continuum.

ACKNOWLEDGMENTS

J.P.R.-A is grateful for the funding of FONDECYT Postdoc. Grant No. 3190301 (2019). P.A.O. acknowledges support from FONDECYT Grant No. 1180914. E.V. thanks the Brazilian agencies CAPES, CNPq, and FAPEMIG for support.

APPENDIX: QD GREEN'S FUNCTION

In this Appendix, we show the procedure used to reach an analytic expression for the QD retarded Green's function in our system. We considered the equation of motion method up to the equations hierarchy that allows describing the Coulomb

blockade phenomena in the QD. The system Hamiltonian is given by Eq. (1). Note that it is not symmetrical in spin degree of freedom, since only continuum electrons with spin $\sigma = \downarrow$ are coupled to the MBS [Eq. (5)]. The general expression for the retarded Green's function equation of motion in the energy domain is given by

$$(\varepsilon + i0^+) \langle \langle A; B \rangle \rangle_\varepsilon^r = \langle \langle A; B \rangle \rangle + \langle \langle [A; H]; B \rangle \rangle_\varepsilon^r, \quad (\text{A1})$$

where A and B are two arbitrary operators, and 0^+ an infinitesimal (positive) number. Throughout this section, as in the main text, we display the energy as $\varepsilon + i0^+ \rightarrow \varepsilon$ for simplicity.

Using Eq. (A1), for spin $\sigma = \downarrow$ electrons, calculating the corresponding commutators/anticommutators, the first hierarchy of equations are

$$(\varepsilon - \varepsilon_d) \langle \langle d_\downarrow; d_\downarrow^\dagger \rangle \rangle_\varepsilon = 1 + \sum_{\mathbf{k}} V \langle \langle c_{\mathbf{k},\downarrow}; d_\downarrow^\dagger \rangle \rangle_\varepsilon + U \langle \langle n_\uparrow d_\downarrow; d_\downarrow^\dagger \rangle \rangle_\varepsilon, \quad (\text{A2})$$

$$(\varepsilon - \varepsilon_{\mathbf{k}}) \langle \langle c_{\mathbf{k},\downarrow}; d_\downarrow^\dagger \rangle \rangle_\varepsilon = V \langle \langle d_\downarrow; d_\downarrow^\dagger \rangle \rangle_\varepsilon - \lambda \langle \langle \gamma_1; d_\downarrow^\dagger \rangle \rangle_\varepsilon, \quad (\text{A3})$$

$$\varepsilon \langle \langle \gamma_1; d_\downarrow^\dagger \rangle \rangle_\varepsilon = -2\lambda \sum_{\mathbf{k}'} \langle \langle c_{\mathbf{k}',\downarrow}; d_\downarrow^\dagger \rangle \rangle_\varepsilon - \langle \langle c_{\mathbf{k}',\downarrow}^\dagger; d_\downarrow^\dagger \rangle \rangle_\varepsilon, \quad (\text{A4})$$

$$(\varepsilon + \varepsilon_{\mathbf{k}}) \langle \langle c_{\mathbf{k},\downarrow}^\dagger; d_\downarrow^\dagger \rangle \rangle_\varepsilon = -V \langle \langle d_\downarrow^\dagger; d_\downarrow^\dagger \rangle \rangle_\varepsilon + \lambda \langle \langle \gamma_1; d_\downarrow^\dagger \rangle \rangle_\varepsilon, \quad (\text{A5})$$

$$(\varepsilon + \varepsilon_d) \langle \langle d_\downarrow^\dagger; d_\downarrow^\dagger \rangle \rangle_\varepsilon = -\sum_{\mathbf{k}} V \langle \langle c_{\mathbf{k},\downarrow}^\dagger; d_\downarrow^\dagger \rangle \rangle_\varepsilon - U \langle \langle n_\uparrow d_\downarrow^\dagger; d_\downarrow^\dagger \rangle \rangle_\varepsilon, \quad (\text{A6})$$

where we have suppressed the superscript r for simplicity. As a consequence of MBS presence, an anomalous Green's function must be calculated. The next hierarchy of equations is extracted from the last terms in Eqs. (A2) and (A6). They lead to

$$(\varepsilon - \varepsilon_d - U) \langle \langle n_\uparrow d_\downarrow; d_\downarrow^\dagger \rangle \rangle_\varepsilon = \langle n_\uparrow \rangle + \sum_{\mathbf{k}} V \langle \langle n_\uparrow c_{\mathbf{k},\downarrow}; d_\downarrow^\dagger \rangle \rangle_\varepsilon + \sum_{\mathbf{k}} V \langle \langle d_\downarrow^\dagger c_{\mathbf{k},\uparrow} d_\downarrow; d_\downarrow^\dagger \rangle \rangle_\varepsilon - \sum_{\mathbf{k}} V \langle \langle c_{\mathbf{k},\uparrow}^\dagger d_\uparrow d_\downarrow; d_\downarrow^\dagger \rangle \rangle_\varepsilon, \quad (\text{A7})$$

$$(\varepsilon + \varepsilon_d + U) \langle \langle n_\uparrow d_\downarrow^\dagger; d_\downarrow^\dagger \rangle \rangle_\varepsilon = -\sum_{\mathbf{k}} V \langle \langle n_\uparrow c_{\mathbf{k},\downarrow}^\dagger; d_\downarrow^\dagger \rangle \rangle_\varepsilon + \sum_{\mathbf{k}} V \langle \langle d_\downarrow^\dagger c_{\mathbf{k},\uparrow} d_\downarrow^\dagger; d_\downarrow^\dagger \rangle \rangle_\varepsilon - \sum_{\mathbf{k}} V \langle \langle c_{\mathbf{k},\uparrow}^\dagger d_\uparrow d_\downarrow^\dagger; d_\downarrow^\dagger \rangle \rangle_\varepsilon. \quad (\text{A8})$$

Up to this point, it is possible to reach the Coulomb blockade regime. Employing the Hubbard approximation, Eqs. (A7) and (A8) can be seen as follows

$$(\varepsilon - \varepsilon_d - U) \langle \langle n_\uparrow d_\downarrow; d_\downarrow^\dagger \rangle \rangle_\varepsilon = \langle n_\uparrow \rangle + \sum_{\mathbf{k}} V \langle n_\uparrow \rangle \langle \langle c_{\mathbf{k},\downarrow}; d_\downarrow^\dagger \rangle \rangle_\varepsilon, \quad (\text{A9})$$

$$(\varepsilon + \varepsilon_d + U) \langle \langle n_\uparrow d_\downarrow^\dagger; d_\downarrow^\dagger \rangle \rangle_\varepsilon = -\sum_{\mathbf{k}} V \langle n_\uparrow \rangle \langle \langle c_{\mathbf{k},\downarrow}^\dagger; d_\downarrow^\dagger \rangle \rangle_\varepsilon, \quad (\text{A10})$$

where we have considered $\sum_{\mathbf{k}} \langle d_\sigma^\dagger c_{\mathbf{k},\sigma} \rangle = \sum_{\mathbf{k}} \langle c_{\mathbf{k},\sigma}^\dagger d_\sigma \rangle$. Replacing Eq. (A10) into Eq. (A6), we have

$$(\varepsilon + \varepsilon_d) \langle \langle d_\downarrow^\dagger; d_\downarrow^\dagger \rangle \rangle_\varepsilon = -\left(1 - \frac{U \langle n_\uparrow \rangle}{\varepsilon + \varepsilon_d + U}\right) \sum_{\mathbf{k}} V \langle \langle c_{\mathbf{k},\downarrow}^\dagger; d_\downarrow^\dagger \rangle \rangle_\varepsilon, \quad (\text{A11})$$

thus, including this result into Eq. (A5), we obtain

$$\left[1 - \frac{V^2 \tilde{g}(\varepsilon)}{\varepsilon + \varepsilon_d} \left(1 - \frac{U \langle n_\uparrow \rangle}{\varepsilon + \varepsilon_d + U}\right)\right] \sum_{\mathbf{k}} \langle \langle c_{\mathbf{k},\downarrow}^\dagger; d_\downarrow^\dagger \rangle \rangle_\varepsilon = \lambda \tilde{g}(\varepsilon) \langle \langle \gamma_1; d_\downarrow^\dagger \rangle \rangle_\varepsilon, \quad (\text{A12})$$

where we have defined $\tilde{g}(\varepsilon) = \sum_{\mathbf{k}} (\varepsilon + \varepsilon_{\mathbf{k}})^{-1}$. Then, the Eq. (A4) is rewritten as

$$\left(\varepsilon - 2\lambda^2 \tilde{g}(\varepsilon) \left[1 - \frac{V^2 \tilde{g}(\varepsilon)}{\varepsilon + \varepsilon_d} \left(1 - \frac{U \langle n_\uparrow \rangle}{\varepsilon + \varepsilon_d + U}\right)\right]^{-1}\right) \langle \langle \gamma_1; d_\downarrow^\dagger \rangle \rangle_\varepsilon = -2\lambda \sum_{\mathbf{k}} \langle \langle c_{\mathbf{k},\downarrow}; d_\downarrow^\dagger \rangle \rangle_\varepsilon. \quad (\text{A13})$$

Consequently, Eq. (A3) is expressed as

$$\left(1 - 2\lambda^2 g(\varepsilon) \left[\varepsilon - \frac{2\lambda^2 \tilde{g}(\varepsilon)}{1 - \frac{V^2 \tilde{g}(\varepsilon)}{\varepsilon + \varepsilon_d} \left(1 - \frac{U \langle n_\uparrow \rangle}{\varepsilon + \varepsilon_d + U}\right)}\right]^{-1}\right) \sum_{\mathbf{k}} \langle \langle c_{\mathbf{k},\downarrow}; d_\downarrow^\dagger \rangle \rangle_\varepsilon = V g(\varepsilon) \langle \langle d_\downarrow; d_\downarrow^\dagger \rangle \rangle_\varepsilon, \quad (\text{A14})$$

defining $g(\varepsilon) = \sum_{\mathbf{k}} (\varepsilon - \varepsilon_{\mathbf{k}})^{-1}$. On the other hand, after replacing Eq. (A9) into Eq. (A2) we obtain

$$(\varepsilon - \varepsilon_d) \langle \langle d_\downarrow; d_\downarrow^\dagger \rangle \rangle_\varepsilon = 1 + \frac{U \langle n_\uparrow \rangle}{\varepsilon - \varepsilon_d - U} + \left(1 + \frac{U \langle n_\uparrow \rangle}{\varepsilon - \varepsilon_d - U}\right) \sum_{\mathbf{k}} V \langle \langle c_{\mathbf{k},\downarrow}; d_\downarrow \rangle \rangle_\varepsilon, \quad (\text{A15})$$

which allows a closed solution for the set of equations. Finally, performing algebraic manipulations we have

$$\langle \langle d_\downarrow; d_\downarrow^\dagger \rangle \rangle_\varepsilon = \frac{\varepsilon - \varepsilon_d - U(1 - \langle n_\uparrow \rangle)}{(\varepsilon - \varepsilon_d)(\varepsilon - \varepsilon_d - U) - \frac{(\varepsilon - \varepsilon_d - U(1 - \langle n_\uparrow \rangle))V^2 g(\varepsilon)}{1 - M(\varepsilon)}}, \quad (\text{A16})$$

where

$$M(\varepsilon) = 2\lambda^2 g(\varepsilon) \left[\varepsilon - \frac{2\lambda^2 \tilde{g}(\varepsilon)(\varepsilon + \varepsilon_d)(\varepsilon + \varepsilon_d + U)}{(\varepsilon + \varepsilon_d)(\varepsilon + \varepsilon_d + U) - V^2 \tilde{g}(\varepsilon)(\varepsilon + \varepsilon_d + U(1 - \langle n_\uparrow \rangle))}\right]^{-1}. \quad (\text{A17})$$

At this point, it is interesting to note that the quantities $V^2 g(\varepsilon)$ and $\lambda^2 g(\varepsilon)$ can be treated within the wide-band approximation. In this limit, they are energy independent and fulfill electron-hole symmetry, such as

$$V^2 g(\varepsilon) = V^2 \tilde{g}(\varepsilon) = -i\Gamma, \quad (\text{A18})$$

$$\lambda^2 g(\varepsilon) = \lambda^2 \tilde{g}(\varepsilon) = -i\Lambda. \quad (\text{A19})$$

Then, the QD Green's function for $\sigma = \downarrow$ is given by

$$\langle \langle d_\downarrow; d_\downarrow^\dagger \rangle \rangle_\varepsilon = \frac{\varepsilon - \varepsilon_d - U(1 - \langle n_\uparrow \rangle)}{(\varepsilon - \varepsilon_d)(\varepsilon - \varepsilon_d - U) - (\varepsilon - \varepsilon_d - U(1 - \langle n_\uparrow \rangle))\Sigma_\downarrow(\varepsilon)}, \quad (\text{A20})$$

where $\Sigma_\downarrow(\varepsilon) = -i\Gamma/[1 - M(\varepsilon)]$ and the whole MBS contribution is embedded in the function

$$M(\varepsilon) = -2i\Lambda \left[\varepsilon + \frac{2i\Lambda(\varepsilon + \varepsilon_d)(\varepsilon + \varepsilon_d + U)}{(\varepsilon + \varepsilon_d)(\varepsilon + \varepsilon_d + U) + i\Gamma(\varepsilon + \varepsilon_d + U(1 - \langle n_\uparrow \rangle))}\right]^{-1}. \quad (\text{A21})$$

For the component $\sigma = \uparrow$, we note that up to the hierarchy considered in this paper, there is no MBS explicit contribution in the corresponding Green's function. Therefore, it can be obtained from Eq. (A20) by fixing $\lambda = \Lambda = M(\varepsilon) = 0$, then $\Sigma_\uparrow(\varepsilon) = -i\Gamma$ and

$$\langle \langle d_\uparrow; d_\uparrow^\dagger \rangle \rangle_\varepsilon = \frac{\varepsilon - \varepsilon_d - U(1 - \langle n_\downarrow \rangle)}{(\varepsilon - \varepsilon_d)(\varepsilon - \varepsilon_d - U) - (\varepsilon - \varepsilon_d - U(1 - \langle n_\downarrow \rangle))\Sigma_\uparrow(\varepsilon)}. \quad (\text{A22})$$

[1] F. Wilczek, *Nat. Phys.* **5**, 614 (2009).

[2] E. Majorana, *Il Nuovo Cimento* **14**, 171 (1937).

[3] N. Read and D. Green, *Phys. Rev. B* **61**, 10267 (2000).

[4] D. A. Ivanov, *Phys. Rev. Lett.* **86**, 268 (2001).

[5] L. Fu and C. L. Kane, *Phys. Rev. Lett.* **100**, 096407 (2008).

[6] A. Kitaev, *Ann. Phys.* **303**, 2 (2003).

[7] A. R. Akhmerov, *Phys. Rev. B* **82**, 020509(R) (2010).

[8] J. Alicea, Y. Oreg, G. Refael, F. von Oppen, and M. P. A. Fisher, *Nat. Phys.* **7**, 412 (2011).

[9] J. Alicea, *Nature (London)* **531**, 177 (2016).

[10] A. Y. Kitaev, *Phys. Usp.* **44**, 131 (2001).

[11] J. Alicea, *Phys. Rev. B* **81**, 125318 (2010).

- [12] V. Mourik, K. Zuo, S. M. Frolov, S. R. Plissard, E. P. A. M. Bakkers, and L. P. Kouwenhoven, *Science* **336**, 1003 (2012).
- [13] M. T. Deng, C. L. Yu, G. Y. Huang, M. Larsson, P. Caroff, and H. Q. Xu, *Nano Lett.* **12**, 6414 (2012).
- [14] A. Das, Y. Ronen, Y. Most, Y. Oreg, M. Heiblum, and H. Shtrikman, *Nat. Phys.* **8**, 887 (2012).
- [15] H. O. H. Churchill, V. Fatemi, K. Grove-Rasmussen, M. T. Deng, P. Caroff, H. Q. Xu, and C. M. Marcus, *Phys. Rev. B* **87**, 241401 (2013).
- [16] S. M. Albrecht, A. P. Higginbotham, M. Madsen, F. Kuemmeth, T. S. Jespersen, J. Nygård, P. Krogstrup, and C. M. Marcus, *Nature (London)* **531**, 206 (2016).
- [17] M. T. Deng, S. Vaitiekėnas, E. B. Hansen, J. Danon, M. Leijnse, K. Flensberg, J. Nygård, P. Krogstrup, and C. M. Marcus, *Science* **354**, 1557 (2016).
- [18] E. J. H. Lee, X. Jiang, R. Aguado, G. Katsaros, C. M. Lieber, and S. De Franceschi, *Phys. Rev. Lett.* **109**, 186802 (2012).
- [19] C. Nayak, S. H. Simon, A. Stern, M. Freedman, and S. Das Sarma, *Rev. Mod. Phys.* **80**, 1083 (2008).
- [20] D. Roy, C. J. Bolech, and N. Shah, *Phys. Rev. B* **86**, 094503 (2012).
- [21] J. D. Cifuentes and Luis G. G. V. Dias da Silva, *Phys. Rev. B* **100**, 085429 (2019).
- [22] J. P. Ramos-Andrade, D. Zambrano, and P. A. Orellana, *Ann. Phys.* **531**, 1800498 (2019).
- [23] J. P. Ramos-Andrade, P. A. Orellana, and S. E. Ulloa, *J. Phys. Condens. Matter* **30**, 045301 (2018).
- [24] A. Schuray, L. Weithofer, and P. Recher, *Phys. Rev. B* **96**, 085417 (2017).
- [25] C.-X. Liu, J. D. Sau, T. D. Stanescu, and S. Das Sarma, *Phys. Rev. B* **96**, 075161 (2017).
- [26] J. F. Silva and E. Vernek, *J. Phys. Condens. Matter* **28**, 435702 (2016).
- [27] D. E. Liu and H. U. Baranger, *Phys. Rev. B* **84**, 201308(R) (2011).
- [28] E. Vernek, P. H. Penteado, A. C. Seridonio, and J. C. Egues, *Phys. Rev. B* **89**, 165314 (2014).
- [29] Note that although QD is not directly connected to the MBS it is close enough so that the local nature of the Majorana wave function is still probed [41].
- [30] J. von Neumann and E. Wigner, *Phys. Z* **30**, 465 (1929).
- [31] C. W. Hsu, B. Zhen, A. D. Stone, J. D. Joannopoulos, and M. Soljačić, *Nat. Rev. Mat.* **1**, 16048 (2016).
- [32] J. P. Ramos and P. A. Orellana, *Phys. B* **455**, 66 (2014).
- [33] M. L. Ladrón de Guevara and P. A. Orellana, *Phys. Rev. B* **73**, 205303 (2006).
- [34] L. S. Ricco, Y. Marques, F. A. Dessotti, R. S. Machado, M. de Souza, and A. C. Seridonio, *Phys. Rev. B* **93**, 165116 (2016).
- [35] L. H. Guessi, F. A. Dessotti, Y. Marques, L. S. Ricco, G. M. Pereira, P. Menegasso, M. de Souza, and A. C. Seridonio, *Phys. Rev. B* **96**, 041114 (2017).
- [36] D. Zambrano, J. P. Ramos-Andrade, and P. A. Orellana, *J. Phys.: Condens. Matter* **30**, 375301 (2018).
- [37] M. Cheng, R. M. Lutchyn, and S. Das Sarma, *Phys. Rev. B* **85**, 165124 (2012).
- [38] M.-T. Deng, S. Vaitiekėnas, E. Prada, P. San-Jose, J. Nygård, P. Krogstrup, R. Aguado, and C. M. Marcus, *Phys. Rev. B* **98**, 085125 (2018).
- [39] C. Lacroix, *J. Phys. F: Metal Phys.* **11**, 2389 (1981).
- [40] F. D. M. Haldane, *J. Phys. C: Solid State Phys.* **11**, 5015 (1978).
- [41] J. Klinovaja and D. Loss, *Phys. Rev. B* **86**, 85408 (2012).